ScientificScholar®
Knowledge is power
Publisher of Scientific Journals

www.clinicalimagingscience.org

Journal of Clinical Imaging Science

Diagnostic Radiology *Review Article*

Acute pelvic pain: A pictorial review with magnetic resonance imaging

Dheeraj Reddy Gopireddy[1], Mayur Virarkar[1], Sindhu Kumar[1], Sai Swarupa Reddy Vulasala[1], Chidi Nwachukwu[1], Sanjay Lamsal[1]

[1]Department of Radiology, UF College of Medicine-Jacksonville, Jacksonville, Florida, United States.

***Corresponding author:**
Sai Swarupa Reddy Vulasala, Department of Radiology, UF College of Medicine-Jacksonville, Jacksonville, Florida, United States.

vulasalaswarupa@gmail.com

Received : 23 June 2022
Accepted : 22 July 2022
Published : 17 August 2022

DOI
10.25259/JCIS_70_2022

Quick Response Code:

ABSTRACT

Acute uterine emergencies constitute both obstetric and gynecologic conditions. The superior image resolution, superior soft-tissue characterization, and lack of ionizing radiation make magnetic resonance imaging (MRI) preferable over ultrasonography (USG) and computed tomography (CT) in investigating uterine emergencies. Although USG is the first-line imaging modality and is easily accessible, it has limitations. USG is an operator dependent and limited by patient factors such as obesity and muscle atrophy. CT is limited by its risk of teratogenicity in pregnant females, poor tissue differentiation, and radiation effect. The non-specific findings on CT may lead to misinterpretation of the pathology. MRI overcomes all these limitations and is emerging as the most crucial imaging modality in the emergency room (ER). The evolving 3D MR sequences further reduce the acquisition times, expanding its ER role. Although MRI is not the first-line imaging modality, it is a problem-solving tool when the ultrasound and CT are inconclusive. This pictorial review discusses the various MRI techniques used in uterine imaging and the appearances of distinct etiologies of uterine emergencies across different MRI sequences.

Keywords: Uterine emergency, Magnetic resonance imaging, Acute pelvic pain, Imaging of pelvic inflammatory disease, Uterine imaging

INTRODUCTION

Uterine emergencies can be categorized into obstetric and gynecologic etiologies. The presentation may be acute or acute on chronic lower abdominal pain with or without vaginal bleeding. Various uterine emergency etiologies and their magnetic resonance imaging (MRI) features are listed in [Tables 1 and 2]. Abnormal uterine bleeding (AUB) is the most common presentation in 1/3rd of patients after acute pelvic pain.[1] Although transvaginal, the US allows for the examination of the internal structures of the uterus, its inability to demonstrate the zonal anatomy and tissue characterization is a significant drawback. MRI is superior to ultrasound and CT in the ancillary description of uterine pathologies in patients presenting to the emergency department with acute pelvic pain and genital bleeding. MR is an emerging modality for various reasons, such as exquisite soft-tissue resolution, its capability of multiplanar imaging, characterization, high sensitivity, and lack of ionizing radiation.[1,2] The sensitivity of MRI in identifying acute uterine pathologies is 96.6%.[3] The knowledge of clinical presentation and imaging appearances of discrete emergent uterine conditions is necessary for a radiologist to arrive at a diagnosis. This pictorial review of MR imaging increases familiarity with the characterization and recognition of acute uterine emergencies.

Table 1: Etiology of uterine emergency.

Non-obstetric causes	Obstetric causes
Pelvic inflammatory disease	Ectopic pregnancy
Endometritis	Molar pregnancy (hydatidiform mole)
Cervicitis	Uterine rupture
Salpingo-oophoritis	Uterine inversion
Pyosalpinx	Retained products of conception
Tubo-ovarian abscess	Placenta accreta spectrum
Leiomyoma	Placental abruption
Torsion	Iatrogenic
Red degeneration	
Adenomyosis	
Endometriosis	
Endometrial polyps and carcinoma	
Uterine arteriovenous malformations	
Pelvic congestion syndrome	
Adnexal torsion	

Before recognizing pathologies on imaging sequences, a thorough understanding of the various techniques and sequences of MRI, along with appearances of typical uterine structures on MRI, is necessary for an accurate approach and assessment of uterine emergencies.

MRI TECHNIQUES

High-field strength MRI with phased array surface coils is used in imaging the female pelvis and uterus. These coils help in increasing the signal-to-noise ratio, thereby providing higher spatial resolution due to the small field of view imaging. Basic pelvic imaging protocol must include axial T1WI with and without fat suppression sequences; axial, oblique sagittal, and coronal sections on T2WI. Axial T1WI assesses the contour of the uterus, the surrounding lymph nodes, and the bone marrow. Oblique axial aids in differentiating the plane between uterine and ovarian masses. The fat suppression sequences assist in determining the fat-containing pelvic masses from the hemorrhagic or proteinaceous masses.

T2WI distinct the zonal anatomy as described below. Sagittal T2WI helps determine the uterus long-axis orientation, which helps evaluate congenital uterine anomalies. To appreciate the anomalies best, the imaging should be taken first in the sagittal axis and then parallel to the long uterine axis that shows the outer uterine contour. The plane imaging of the short axis of the cervix best evaluates the extent of parametrial invasion in the cervical cancer.[4] Even though fast breath-hold sequences provide reduced resolution, they usually suffice for evaluating benign diseases. However, fast spin-echo (FSE) T2 WI sequences with long duration and high resolution are required for malignancies.

Sequences other than T1WI and T2WI include diffusion-weighted imaging (DWI), dynamic contrast-enhanced (DCE) MRI, peristalsis, and pelvic floor imaging. These are usually employed in assessing the extent of malignancy, recurrence, and therapeutic outcomes.[5,6] The DWI allows tissue characterization by deriving the image contrast from the molecular Brownian motion. The degree of diffusion restriction is inversely related to the continuity of cell membranes and high cellular density. The lesions with restricted diffusion are hyperintense on DWI and hypointense on apparent diffusion coefficient (ADC) maps. Contrast-enhanced magnetic resonance angiography is a modality available for assessing uterine vasculature or evaluating vascular pathologies. Susceptibility-weighted imaging increases magnetic susceptibility effects such as "signal voids" and is extremely sensitive to blood products.[7] 3D-SPACE sequence imaging allows for multiplanar reconstruction of images obtained in a single plane without compromising image quality and diagnostic information. It significantly reduces the acquisition time compared to the time taken for 2D sequences taken in axial, coronal, and sagittal planes. Hence, 3D SPACE is rapid and effective imaging for urgently actionable conditions.[4]

During pregnancy, the non-ionizing radiation used in MRI causes tissue heating in the fetus, effects on acoustic noise, and energy deposition. The energy deposition is termed a "specific absorption rate." FSE echo sequences have a higher specific absorption rate than gradient-echo sequences.[8] To minimize these risks, MRI with a field strength of 1.5T or less is used in pregnant patients.[9] As per FDA, gadolinium is considered a category C drug in pregnancy, meaning that it should be used only when it is crucial to perform contrast imaging for evaluation.[9] The anatomical artifact during female pelvic imaging concedes the diagnostic features. An antispasmodic agent's intake of glucagon reduces the bowel movement artifacts and improves imaging quality. Furthermore, fasting for at least 4 h and adopting saturation bands during imaging increase the rate without affecting turnaround time.[10] The entire bladder diminishes the fat plane between bladder and uterus, resulting in difficulty assessing the bladder involvement in the direct metastatic spread of adjacent carcinomas. Hence, moderately filled bladder is recommended in the female pelvic imaging.[10]

NORMAL MRI ANATOMY OF UTERUS AND ADNEXA

Uterus

Zonal anatomy of the uterus includes endometrium and myometrium. The myometrium further divides into inner and outer layers. The differentiation of layers is

Table 2: MR imaging features of uterine emergencies.

Etiology	T1WI	T2WI	Gd enhanced	Comments/additional imaging findings
Cervicitis/ endometritis	Enlarged uterine cervix with enhanced endocervical canal	Enlarged uterus with hyperintense endometrium	Intense uterine enhancement secondary to hyperemia	MRI is infrequently used in acute PID; may have benefit in complicated chronic PID
Acute salpingitis/ pyosalpinx	Swollen fallopian tube with low signal intensity in acute salpingitis and variable signal intensity in pyosalpinx	Intermediate to high signal intensity	Mural hyperenhancement may be observed	"Waist sign" and "cogwheel sign" on imaging are specific to pyosalpinx
Tubo-ovarian abscess	Heterogeneous low signal intensity with high signal intensity rim	Heterogeneous high signal intensity with multiple low signal septa	Rim and septal enhancement	Diffusion restriction on DWI.
Leiomyoma	Intermediate signal intensity; submucosal fibroid appears as a bulky mass protruding through the cervix ("Broccoli sign")	Low signal intensity compared to myometrium	Homogeneous enhancement	Most accurate modality to detect and characterize the fibroids; helpful in cases of inconclusive ultrasound for surgical management
Red degenerated fibroids	Diffuse or peripheral hyperintensity due to methemoglobin	Variable signal intensity and hypointense rim due to hemosiderin deposition	Less marked or absent enhancement	MRI aids in differentiating leiomyoma and leiomyosarcoma
Adenomyosis	Intermittent high signal intensity representing hemorrhage and endometrial glands	Hypointense smooth muscle and hyperintense endometrial glands	Does not aid in diagnosis	Mimics/pitfalls of MRI in adenomyosis: Proliferative phase, postmenopausal phase, and anti-contraceptive use effects on junctional anatomy; transient uterine contractions; endometrial pseudo-widening
Endometrial polyp	Isointense to endometrium	Sessile or pedunculated mass with hypointense central fibrous core surrounded by hyperintense fluid and endometrium	Early persistent or gradual increase in enhancement similar to or greater than outer myometrium	Intermediate to low choline peak on MR spectroscopy
Pelvic congestion syndrome	Hypointense flow voids on angiography	Hyperintense veins with reduced flow velocity	Retrograde caudal filling of gonadal veins and early emptying of pelvic veins into iliac veins on late-phase MRI	Compared to venography, MR angiography has higher sensitivity in identifying congestion.
Ectopic pregnancy	Cystic gestational sac with intermediate to high SI	Heterogeneous or predominantly high SI mass appearing as a thick-walled ring	Enhancing solid components are observed	Various MRI sequences such as fat-suppression HASTE, breath-hold HASTE and GRE aids in differentiation between acute appendicitis and ectopic pregnancy

(*Contd*...)

Table 2: (*Continued*).

Etiology	T1WI	T2WI	Gd enhanced	Comments/additional imaging findings
Molar pregnancy/ gestational trophoblastic disease	Ill-defined or sharply marginated isointense mass relative to myometrium	Hyperintense mass relative to myometrium	Avidly enhancing mass	MRI is superior to ultrasound in evaluating extrauterine tumor extension
Uterine rupture	High signal foci suggestive of proteinaceous blood contents	Lower T2 signal intensity ratio is associated with abnormal uterine scar		MRI aids in visualizing serosal layer to differentiate between uterine dehiscence and rupture.
Uterine inversion	T1WI is not informative in uterine inversion	U-shaped uterus with indented fundus on sagittal imaging; Bull's-eye configuration on axial imaging		MRI confirms the diagnosis in patients with inconclusive ultrasound findings
RPOC	Polypoid mass in endometrium with low signal intensity	Mass in the endometrium with high signal intensity	Heterogeneous enhancement	MRI features of RPOC overlap with gestational trophoblastic disease

RPOC: Retained products of conception, PID: Pelvic inflammatory disease

best depicted in T2WI. On T1WI, the signal intensity of the uterus is like the surrounding muscle. Hence, it does not help distinguish zonal anatomy. On T2WI, the endometrium appears hyperintense due to mucin-rich endometrial glands and matrix. The thickness varies depending on menarcheal status and the menstrual cycle phase. The thickness range in premenopausal women is 1 mm–16 mm, with a steady increase in the thickness from the follicular phase to the secretory phase. Sheik-Sarraf *et al*. reported that the phase-dependent variation of the endometrium is not significant.[10] In postmenopausal women, >5 mm is considered abnormal if the patient has AUB or >9 mm in the case of asymptomatic patients.[1] On DWI, the endometrium is visualized as a hyperintense layer due to high water content in the stromal cells and the "T2 shine-through effect."[11] The T2 shine-through effect refers to high signal intensity on DWI that is not due to diffusion restriction but due to high T2 signal that occurs in normal tissue because of long T2 decay. The inner myometrium, called the junctional zone, contains compact muscle with a sparse extracellular matrix. This leads to a hypointense signal on T2WI. The width of the junctional zone is usually <12 mm.[12] As we move from inner to outer myometrium, the muscle component decreases with a rise in the intercellular matrix that contributes to the hyperintense signal on T2WI. This differentiation of zonal anatomy is best evident in the reproductive age group compared to premenarchal and postmenopausal women.[6]

Cervix

On T2WI, an endocervical canal filled with mucus appears hyperintense such as endocervical mucosa containing mucin glands. Both the canal and mucosa constitute 2–3 mm thickness. Surrounding the mucosa, a hypointense layer filled with fibroblasts and smooth muscle cells with little stroma is usually 3–8 mm thick. Increasing stroma content in the next outer layer leads to the intermediate intensity, and the layer is continuous with the outer layer of the uterine myometrium.[5]

Adnexa

The ovaries and fallopian tubes constitute the adnexa. The visualization and interpretation of adnexa are challenging due to the different shapes, volumes, and cyclical alterations. Hence, the knowledge of the anatomy of adnexa plays a crucial role in differentiating normal from pathological abnormalities. Each fallopian tube measures around 10 cm in length and 1 cm in width.[13] The ovarian volume decreases each decade and is around 20 cm^3 in premenopausal women and about 10 cm^3 in postmenopausal women.[14] The Graafian follicles seen in the ovaries grow to a maximum size of 18–20 mm by the mid-cycle and then rupture to release the ovum. If the follicle is not ruptured and grows to a size >3 cm, it is termed a follicular cyst. On MRI, the fallopian tubes are seen as serpentine structures that are intermediate to low signal intensity adjacent to ovaries.[15] The tubal lumen is usually not visible in an average fallopian tube and

is explained by the plicae and involuting normal mucosa in the histology.[15] The ovaries are isointense on T1WI relative to the myometrium. On T2WI, well-distinguished zonal anatomy is seen. The peripheral ovarian cortex appears hypointense, and the central medulla appears hyperintense. These patterns are observed in reproductive-aged women. In the postmenopausal age group, the ovaries appear homogeneously hypointense field as the medulla is replaced by stromal cells.[16] The Graafian follicles in the ovaries appear as hyperintense cysts surrounded by hypointense ovarian stroma.

NON-OBSTETRIC CAUSES

Pelvic inflammatory disease (PID)

PID is an ascending sexually transmitted infection and inflammation of the female genital tract. It is manifested as a syndrome of dull lower abdominal pain, abnormal discharge, dyspareunia, fever, and elevated leukocyte counts.[17] The most common organisms identified in PID are Chlamydia trachomatis and Neisseria gonorrhoeae.[18] Other less common organisms include mycoplasma (14% of cases) and Gram-negative rods.[18] The extent of involvement has endometritis, cervicitis, salpingo-oophoritis, and pelvic soft-tissue inflammation. The acute complications of PID are evidenced as tubo-ovarian abscess, pyosalpinx, pyometra, peritonitis, and perihepatitis (Fitz-Hugh Curtis syndrome). Ultrasound is the first-line imaging and provides a good visualization of PID complications such as an abscess. However, it cannot lead to a definitive diagnosis in contrast to MRI, which is superior in identifying tissue inflammation.[2] MRI is usually reserved when the diagnosis of PID is not conclusive or if there is any suspicion of fistula, torsion, or tumor. MRI has a sensitivity, specificity, and diagnostic accuracy of 95%, 89%, and 93% in diagnosing the PID.[17]

Salpingitis and pyosalpinx

Salpingitis refers to thickened, inflamed, and dilated fallopian tube secondary to the obstructed ampulla, whereas pyosalpinx (tubal abscess) refers to a pus-filled fallopian tube.[1] Salpingitis accounts for a higher risk of infertility and ectopic pregnancies. The causes of ampullary obstruction include prior PID, ectopic pregnancy, or adhesions.[19] The tubal content appears hypointense on T1WI and DWI and hyperintense on T2WI sequences. Post-contrast T1-weighted fast-spin echo in salpingitis demonstrates minimal enhancement of a uniform and thin fallopian tube wall. T2-weighted fast-spin echo shows hyperintense peri-tubal signal indicative of edema. Other MR features suggesting acute salpingitis are a parametrial enhancement, thickening of fascial planes, and pelvic edema [Figure 1]. The affected fallopian tube appears to be a tortuous C- or S-shaped sausage structure due to a tubal folding.[20]

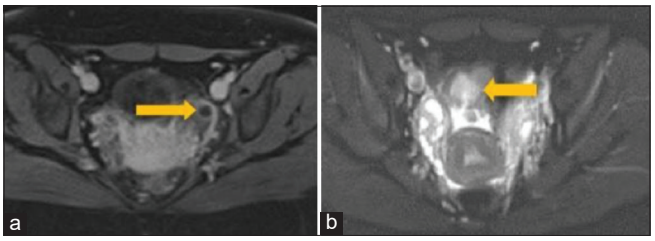

Figure 1: A 48-year-old woman presented with salpingitis presenting with pelvic pain. (a) Axial T1 post-contrast fat saturated shows enhancement of the tubes (arrow) and adnexal fat. (b) Axial T2 fat saturated shows marked high signals in the para uterine soft-tissues (arrow) mesenteric fat with small amounts of fluid.

MRI also aids in distinguishing the tubal mass from the ovarian mass. The pathognomonic feature of hydrosalpinx on MRI is the "cogwheel" appearance of the fallopian tube on cross-sectional imaging due to thickened longitudinal folds.[19] Pyosalpinx demonstrates a shading sign-like endometriomas due to its high-protein content [Figure 2].[12] Differential diagnoses of pyosalpinx include hematosalpinx seen in cases of ectopic pregnancy. The hematosalpinx does not demonstrate thickening of the wall and appears hyperintense due to blood on T1WI.[19] At the same time, pyosalpinx shows variable signal intensity on T1WI. DWI assists in identifying the tubal lumen content. No restricted diffusion indicates hydrosalpinx, and restricted diffusion is suggestive of pyosalpinx or tubo-ovarian abscess.[1] After treatment with appropriate antibiotics, the infection resolves with proteolysis of pus contents, filling the tube with serous fluid.

Tubo-ovarian abscess

The incidence of TOA is around 15% in cases of PID[1] and is unilateral in 25–50% of TOA cases.[21] On MRI, the intensity of abscess varies depending on the blood and protein content [Figure 3].[22] The abscess appears as a hypointense mass on T1WI and a hyperintense complex mass with thick hypointense septa on the T2WI.[1] The vascular granulation tissue best describes the hyperintense and contrast-enhanced rim on T1WI and hemorrhage.[1,12,19] The fat-saturated window increases the intensity of surrounding peritoneal fat, and post-contrast enhancement/visualization of septa and inflammatory stranding are noticed in TOA.

On DWI, the TOA appears as a high signal intensity lesion with low ADC values. The higher the viscosity of pus, the higher the signal intensity on DWI, and the lower the signal intensity on ADC map.[23] These findings, along with high or intermediate signal intensity on T2-weighted imaging sequence and absent enhancement, are the best criteria to determine TOA. Including MRI and DWI findings in the diagnosis increase the diagnostic confidence to 22.5%.[24] The

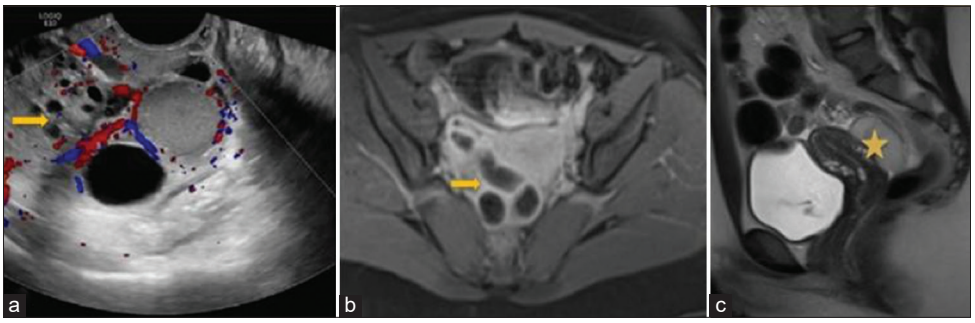

Figure 2: A 39-year-old woman presented with pyosalpinx presenting with abdominal and pelvic pain. (a) Ultrasonography shows an adnexal tubular lesion with internal echoes separate from the ovary (arrow). (b) Axial T1-WI-WI fat-saturated MRI shows dilated right tube (arrow) with enhancing walls and inflammation compatible with pyosalpinx. (c) Sagittal T2 non-fat-saturated MRI shows tubal inflammation (star) in the cul-de-sac with debris.

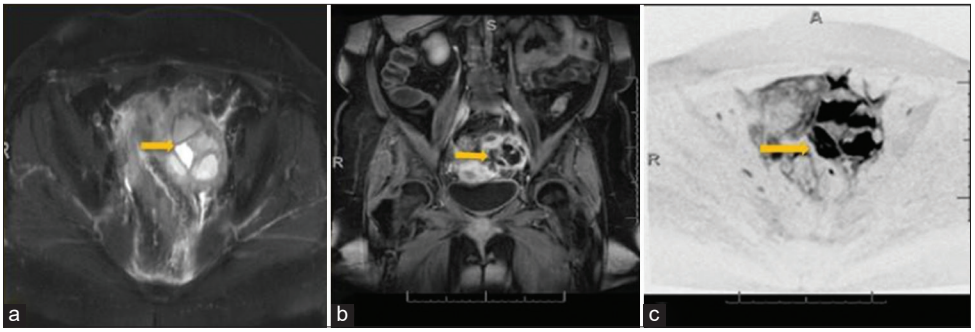

Figure 3: A 47-year-old woman presented with tubo-ovarian abscess presenting with fever and pelvic pain. (a) Axial T2 fat saturated shows marked edematous and enlarged ovary with loculations (arrow). (b) Coronal T1 fat saturated shows enhancing the left ovary with loculations (arrow). (c) Axial DWI shows marked restricted diffusion of the loculations (arrow), supporting abscess formation.

TOA must be distinguished from a pelvic abscess, ovarian epithelial malignancy, and primary fallopian tube carcinoma. The anteriorly displaced broad ligament differentiates TOA from the pelvic abscess.[19] Ovarian epithelial malignancy originates from the ovary and is usually not associated with dilated fallopian tubes. The distinguishing features of primary fallopian tube carcinoma include homogenous mass with hypointensity on T1, hyperintensity on T2, post-contrast enhancement, hydrosalpinx, and fluid in the uterine cavity. The intrauterine fluid is found in 30% of cases of PFTC and is specific to carcinoma. Furthermore, PFTC can be differentiated based on its lower ADC values and higher intensity on DWI.

Leiomyoma

The fibroids or leiomyomas are more common in the reproductive age group, and the incidence is around 20–40% in women above 30 years.[6,20] The acute complications include torsion, prolapse, and degeneration (hyaline, red, myxoid, and cystic). The subserosal fibroids are usually more prone to torsion, whereas submucosal types are prone to prolapse. The degeneration occurs secondary to a lack of vascular supply due to the outgrowth of the tumor. Red or hemorrhagic degeneration presents acutely with severe pelvic pain due to peripheral venous thrombosis.[20] It is seen in pregnancy and patients using oral contraceptive pills.[20]

Leiomyomas appear isointense on T1WI and hypointense with well-defined margins on T2WI compared to the surrounding myometrium [Figures 4 and 5].[5] They enhance homogeneously in the post-contrast imaging.[6] Fibroids should be differentiated from ovarian fibroma and Brenner's tumor, which have similar appearances.[5] According to Thomassin-Naggara *et al*., the DCE-MR enhancement rate is high in leiomyomas compared to ovarian fibromas considering maximal enhancement and enhancement rate at 30, 60, and 90 s.[25] Calcified fibroids are usually seen in older women and may cause a signal void in the imaging.[12] Prolapsed fibroid with its stalk attached to the uterine wall is best visualized on T2WI, and it is described as a "broccoli sign."[20] Interstitial edema, the formal sign of degeneration, appears hyperintense on T2WI and enhances

gadolinium-enhanced T1WI.[26] Hemorrhagic degeneration on MRI shows a central hyperintense signal due to methemoglobin on T1-weighted imaging, and the peripheral hypointense signal is observed on T2WI due to hemosiderin deposition.[1,20] Some leiomyomas demonstrate peripheral hyperintensity on T2WI representing pseudo-capsule (lymphatic vessels, veins, and edema).[27] Post-contrast MRI shows no enhancement due to underlying vascular deficit both in case of torsed and degenerated fibroid.

Adenomyosis

The infiltration of benign ectopic endometrium into the uterine myometrium is termed adenomyosis. The muscle further undergoes diffuse or focal hyperplasia and hypertrophy. The incidence is around 65%.[28] The patient presents with menorrhagia, dysmenorrhea, and lower abdominal pain. The diagnostic accuracy of MRI in adenomyosis is 85%, and it is best depicted on T2WI.

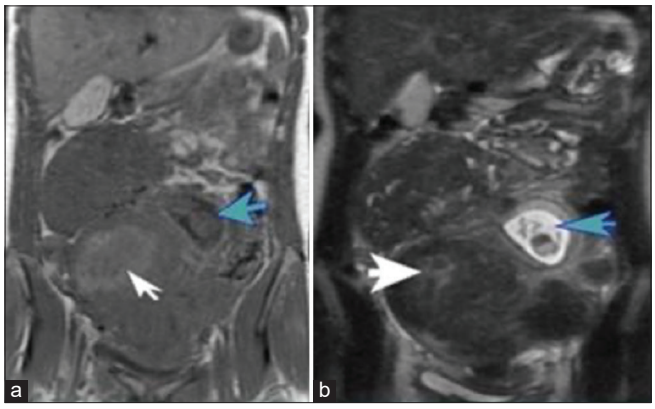

Figure 4: A 41-year-old woman presented with leiomyoma presenting with menstrual irregularities. (a) Coronal T1 non-fat saturated shows multiple fibroids with a fundal fibroid demonstrating a high T1 signal (white arrow) and fetal pole (aqua arrow). (b) Coronal T2 steady-state fast spin-echo (SSFSE) shows a high signal due to edema (white arrow). Notice the fetal pole (blue arrow).

The diffusely increased thickness of the junctional zone to >12 mm is the frequent criterion on MRI to indicate adenomyosis. The compactly arranged smooth muscle produces low signal intensity, and ectopic endometrial glands produce high signal foci on T2WI. Intermittent high signal intensity foci speak for hemorrhage and ectopic endometrial glands on T1WI [Figure 6].[27] Adenomyosis can be differentiated from leiomyomas by its "ill-defined" low-intensity smooth muscle and high-intensity ectopic endometrial glands on T2WI.

Endometriosis

Endometriosis is characterized by the presence of ectopic endometrial tissue outside of the uterus. It is observed among 10% of women of childbearing age and 5% of women in the postmenopausal age group.[29] Endometriosis is often intrapelvic and affects the ovaries, fallopian tubes, peritoneum, uterine ligaments, bladder, and rectovaginal septum. Occasionally, in 1% of cases, it may be seen in the liver, lung, diaphragm, pancreas, abdominal wall, and perineum and poses a diagnostic challenge in such situations.[29] There are three types of endometriosis: (i) Superficial: Located at or <5 mm from the peritoneal surface, (ii) deep: Located 5 mm away from the peritoneal surface or may be invading the wall of adjacent pelvic organs, and (iii) endometriomas: Cystic structures filled with hemorrhagic content. Patients typically present with dysmenorrhea, dyspareunia, and constipation. Although ultrasound is the initial assessment tool for endometriosis, laparoscopy is the gold standard diagnostic and therapeutic procedure. Ultrasound is limited by the operator dependency and relatively small field of view. In the case of inconclusive ultrasound, MRI aids in evaluating endometriosis with a sensitivity and specificity of 69–92% and 75–98%, respectively.[30,31]

The T2WI sequences are most commonly used to assess pelvic endometriosis, while the T1WI with and without fat suppression are suitable to evaluate ovarian endometriomas [Figure 7]. The endometriosis has a heterogeneous signal

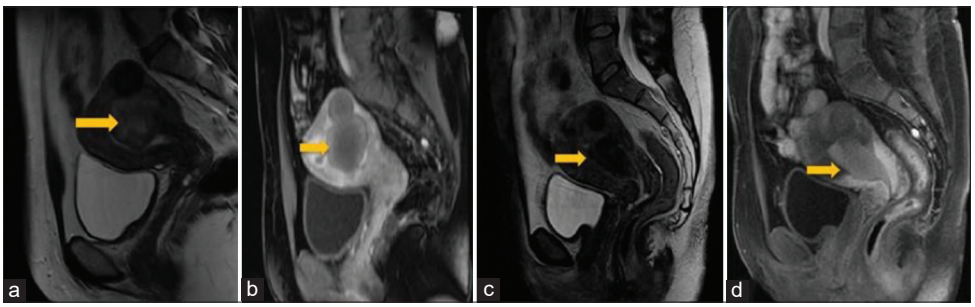

Figure 5: A 52-year-old woman presented with embolized leiomyoma presenting with dyspareunia. (a) Sagittal T2 and (b) post-contrast T1 fat saturated show a large submucosal fibroid before UAE (arrow). (c) Sagittal T2 and (d) post-contrast T1 fat-saturated post-embolization demonstrate sloughing fibroid (arrows).

intensity on T1WI and T2WI depending on the age of hemorrhage. Subacute bleeding has a high signal intensity on T1WI and low signal intensity on T2WI. In the case of chronic recurrent bleeding and reactive fibrosis, MRI depicts dilated endometrial glands with high signal intensity and fibrosis with low signal intensity on T1WI and T2WI. Although gadolinium chelate has no role in deep pelvic endometriosis, it aids in diagnosing atypical adnexal lesions.

Endometriomas present high signal intensity on T1WI secondary to hemorrhage and high-protein content and homogeneously low signal intensity on T2WI secondary to iron and blood accumulation (T2 shading). The T2 shading feature is susceptible (>93%) and has low specificity (45%) in the evaluation of the endometriomas.[32] In such situations, the T2 dark spot sign, characterized by the low signal intensity foci within the cyst cavity, aids in diagnosing with a sensitivity and specificity of 36% and 93%, respectively.[32] The low signal intensity peripheral rim also characterizes endometriomas on T2WI. MRI shows septate cysts filled with papillary projections and solid components in patients with decidualized endometriomas. They demonstrate high signal intensity on T2WI, high ADC values, and the absence of an increased signal on DWI with b values of 1500 s/mm^2.

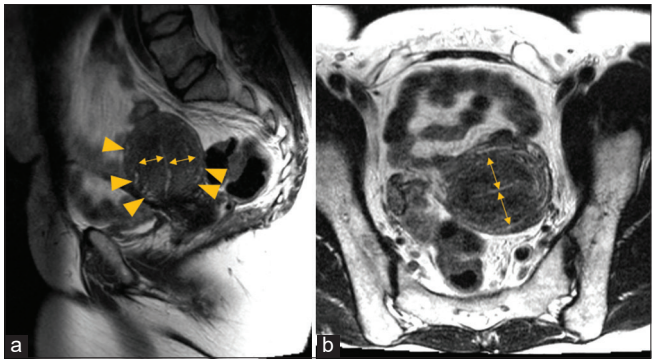

Figure 6: A 31-year-old woman presented with dysmenorrhea from adenomyosis. (a) Sagittal T2-weighted image, (b) axial T2-weighted MRI images show widening of the junctional zone (double head arrows) measures up to 1.7 cm and T2 hyperintensities (arrowheads) consistent with uterine adenomyosis.

Endometrial polyps

Endometrial polyps are sessile or pedunculated endometrial overgrowths containing endometrial stroma, glands, and vascular tissue. Bleeding is the most common presentation of the polyps and is seen in 68% of cases.[33] Although ultrasound is the first-line imaging, it cannot provide differentiation between polyps, endometrial hyperplasia, and endometrial carcinoma, which share the presenting symptoms. Endometrial polyps are isointense to normal endometrium on T1WI, hypointense fibrous stroma surrounded by the hyperintense fluid on T2WI, hypointense on DWI, homogenous moderate enhancement Gd-T1WI, and early enhancement on dynamic MRI [Figure 8]. Polyps of size <5 mm are difficult to distinguish from normal endometrium.[34] Endometrial carcinoma can be classified into two types; Type 1 arises secondary to endometrial hyperplasia and type 2 develops from the atrophic endometrium. The differentiating features of polyp and carcinoma are described in [Table 3].[11]

Uterine arteriovenous malformations (AVMs)

AVMs are uncommon and abnormal communication between arteries and veins bypassing the capillaries. The AVM can be congenital or acquired. The latter is more common than congenital and occurs secondary to tissue trauma like surgery.[35] AVMs constitute 1–2% of all cases presenting with life-threatening vaginal bleeding.[36] AUB and recurrent pregnancy losses are the most common presentations. Angiography is the gold standard investigation that acts as a diagnostic and therapeutic modality.[37] Early venous return on angiography and myometrial involvement is more classic for AVM diagnosis.[38]

MRI detects high-sensitivity AVM and demonstrates multiple, tortuous, serpiginous flow-related signal voids, and prominent para uterine vessels [Figure 9]. AVMs exhibit a polypoid shape when they protrude into the uterine cavity. Other features on MRI include a bulky uterus with a focal tangle of vessels disrupted junctional zone. 3D contrast MR angiography shows coils of uterine blood vessels draining into the parametrial veins, and these findings correlate well with the results of the invasive angiography.[36,37] AVMs involve the myometrial layer,

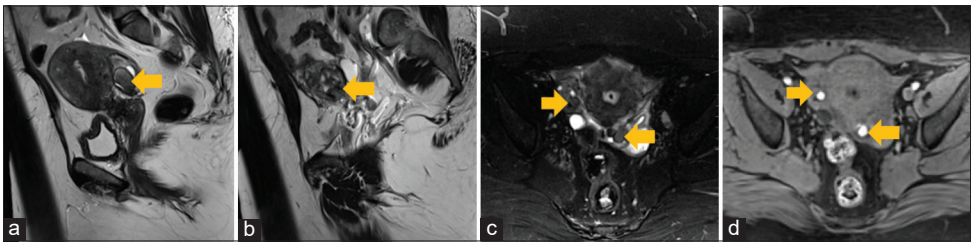

Figure 7: A 36-year-old woman presented with cyclical pelvic pain from endometriosis. (a) Sagittal T2-weighted image (left side), (b) sagittal T2-weighted image (right side), (c) axial T2-weighted image fat saturated, and (d) axial T1-weighted image fat-saturated MRI images demonstrate T1 hyperintense and T2 hypointense bilateral adnexal endometrial implants (arrow) separate from ovaries and consistent with endometriosis.

Table 3: Differentiating MR imaging features of uterine pathology.

Etiology	T1 and T2 WI	Post-contrast T1-WI	DWI
Leiomyoma	Hypointense, well delineated. T1 – High intensity signals may be seen due to fat in cases of lipoleiomyoma or due to infarcted tissue in cases of degenerated leiomyomas.	Early enhancement; Degenerated leiomyomas: Dim enhancement	Lower ADC values except in cases of cystic and myxomatous degeneration where higher ADC values are observed.
Leiomyosarcoma	T1 – Variable intensity heterogeneous mass with hyperintense areas representing hemorrhage and necrosis T2 – Intermediate to high intensity	Early and heterogeneous enhancement with non-enhanced areas corresponding to necrosis	Lower ADC values compared to degenerated leiomyomas
Endometrial polyp	T2 – Hypointense fibrous core and hyperintense smooth-walled intralesional cysts.	Equal or more intense enhancement than myometrial layer	Hypointense compared to normal endometrium
Endometrial carcinoma	T2 – Isointense to myometrium	Type: 1 Less enhanced than myometrium Type: 2 Strong enhancement like polyp	Lower ADC. Hyperintense like normal endometrium

ADC: Apparent diffusion coefficient

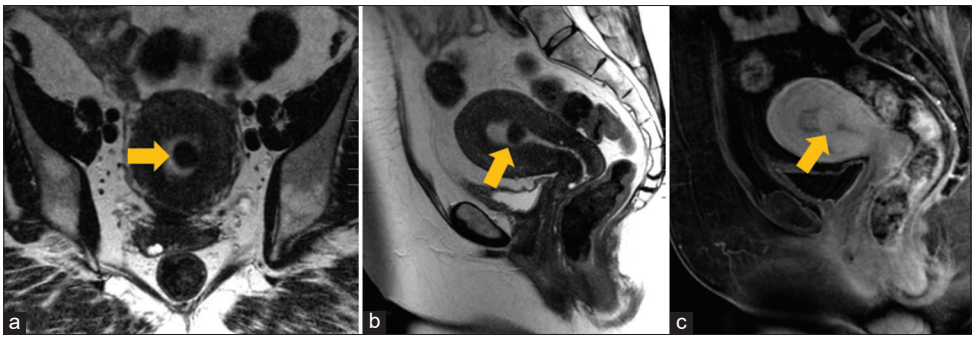

Figure 8: A 38-year-old woman presented with pelvic pain from biopsy-proven endometrial polyp. (a) Axial T2-weighted image, (b) sagittal T2-weighted, and (c) post-contrast sagittal T1-weighted fat-saturated MRI images demonstrate biopsy-proven enhancing endometrial polyp (arrow).

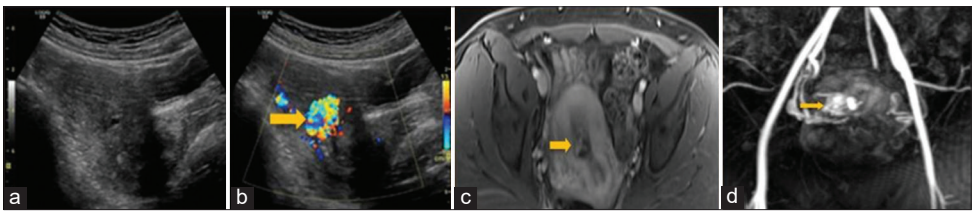

Figure 9: A 48-year-old woman presented with arteriovenous malformations presenting with pelvic pain. (a and b) Ultrasonography and Doppler ultrasonography show aliasing within the cystic area of the myometrium (arrow). (c) Axial T1 post-contrast fat saturated leads serpiginous enhancing vessels (arrow) in the junctional zone. (d) Coronal MRA shows focal serpiginous enhancing vessels in the junctional zone (arrow) AV fistula.

whereas retained products of conception (RPOC) involves the endometrial layer. Proper identification is crucial in preventing life-threatening hemorrhage due to AVMs mistaken for RPOC and treated with dilatation and curettage.[39]

Pelvic venous congestion syndrome (PVCS)

PVCS causes include left renal vein compression by a tumor along with gonadal vein valvular incompetence (Nutcracker syndrome), compressed iliac vein (May-Thurner

configuration), and refluxing into an internal iliac vein on the same side.[40] The patients present with chronic dull pelvic pain, pressure, and heaviness exacerbated during menses, prolonged standing, and activities causing exertion. The imaging diagnosis of PVCS is made when at least one of the four dilated tortuous ipsilateral para uterine veins is >4 mm or an ovarian vein diameter >8 mm.[41] Flow velocity <3 cm/s or presence of reflux scored from 0 to 3 on Doppler ultrasound, or dynamic MR angiography can also be considered a diagnostic.[42,43]

High temporal time-resolved dynamic T2-weighted MR angiography is preferred in PVCS to evaluate reflux in the gonadal vein and pelvic venous collaterals.[40] Compared to venography, it showed a sensitivity of 100%, specificity of 67–75%, and accuracy of 79–84%.[44] T1WI shows hypointense flow voids representing engorged vessels [Figure 10]. On T2WI, hyperintense veins are seen with decreased flow velocity.[41] On T1-weighted gradient echo post-contrast sequence, varices are best visualized in the venous phase. Detection of retrograde caudal filling of gonadal veins, its flow velocity, and early emptying of pelvic veins into iliac veins are seen in late phase arterial MRI.[41] This finding has sensitivity and specificity of 100% and 50%, respectively.[40]

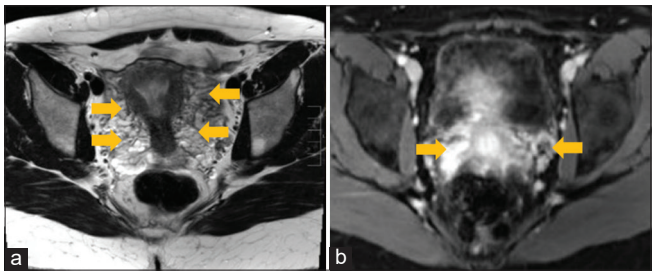

Figure 10: A 45-year-old woman presented with chronic pelvic pain from pelvic congestion syndrome. (a) Axial T2-weighted image, (b) post-contrast axial T1-weighted fat-saturated MRI images show enhancing pelvic and periuterine vessels (arrows) suggestive of pelvic congestion syndrome.

Adnexal torsion

Adnexal torsion is a rare presentation associated with an ipsilateral ovarian tumor or cyst in 50–81% of cases.[45] Of all the ovarian tumors, benign cystic teratoma is frequently associated with torsion and is noticed in 3.5–16.1% of cases.[45] Patients with sudden onset abdominal pain requiring immediate surgical intervention may progress to infarction, infection, peritonitis, and death if the left untreated. US is the first-line imaging modality to assess the patients suspected of acute adnexal torsion. Whereas in subacute to chronic cases, MRI aids in identifying the general configuration of the ovarian infarction. Twisting of the ovarian pedicle is pathognomonic and is observed in <1/3rd of MR images. Multiplanar MRI acquisitions are required to appreciate the twisted pedicle. In a study, tube thickening (84%), smooth wall thickening of ovarian mass (76%), ascites (64%), and uterine deviation to the twisted side (36%) are the most common findings in MR imaging [Figure 11].[45] Tube thickening is best demonstrated on sagittal MR imaging and manifests as a beaklike protrusion from the superiorly located adnexal mass to the inferiorly located uterus. Other features that suggest adnexal torsion include absent enhancement of the solid component, cyst wall, or a mural nodule.

OBSTETRIC CAUSES

Ectopic pregnancy

The incidence of ectopic pregnancies is around 2%.[46] Of which 95% are found in the fallopian tube, with ampulla (75–80%) being the most common implantation site in the tube.[8,38,46] Routine ultrasound with serum beta-HCG is done to diagnose ectopic pregnancy. According to the third international standard, normal intrauterine pregnancy should be visible on USG with serum beta-HCG levels >1000 mIU/mL. However, if the gestational sac is small without fetal cardiac motion or in cases of early-stage ectopic, the diagnosis with USG alone becomes difficult. In such situations with indeterminate ultrasound and

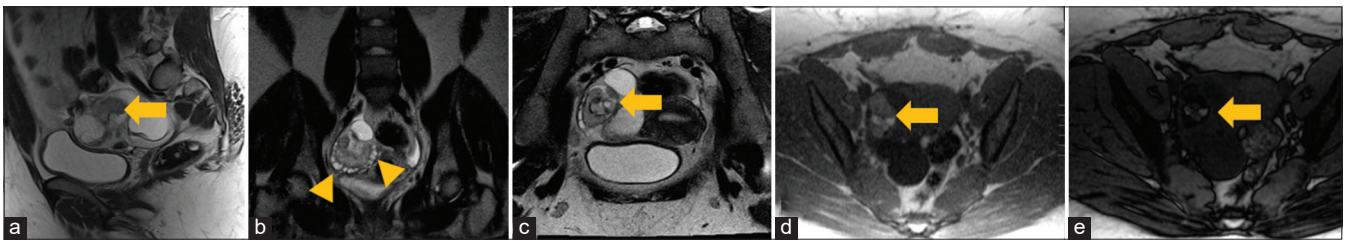

Figure 11: A 31-year-old woman presented with acute pelvic pain from ovarian torsion due to a dermoid. (a) Sagittal T2-weighted image, (b) coronal T2-weighted image, (c) axial oblique T2-weighted image, (d) in-phase, and (e) out-phase MRI images demonstrate enlarged heterogeneous right ovary with a 4.5 cm ovarian teratoma (arrow) along with several additional ovarian cystic lesions (arrowhead). There is a signal dropout on out-of-phase images consistent with intralesional fat. These findings are consistent with ovarian torsion.

increasing beta-HCG, MRI plays a key role in detecting the ectopic and its complications, thereby facilitating immediate management. MRI also aids in evaluating interstitial ectopic pregnancy and pregnancy in Mullerian anomalies, which are challenging to identify on ultrasound.

Axial and coronal T2WI are more helpful in identifying gestational sacs. Tubal pregnancy is seen as a "three rings" cystic saclike structure with a thick hyperintense wall on T2WI.[8,46] The wide middle ring is hyperintense due to chorionic villi. The thin outer ring formed by the tubal wall is hypointense due to hemorrhage. The thin inner ring with coelom and amnion lacking blood vessels appears hypointense on T 2WI.[46,47] On T1WI, intermediate to high intense foci may be seen in the cyst representing hemorrhagic foci. On post-contrast imaging, enhancing solid components are seen in cases of large gestational sacs representing embryonic tissues. These are best identified by T2-weighted 3D fiesta and coronal CUBE T2-weighted fast spin-echo imaging. CUBE imaging takes longer and is preferred in hemodynamically stable cases. Hematosalpinx on MR appears as a dilated tube with wall enhancement. During embryo implantation, penetration of the tubal wall by chorionic villi is responsible for an enhanced wall on imaging. Ruptured ectopic leads to hemoperitoneum, which appears hyperintense on T1WI and variable intensity on T2WI.[8,46]

Few cases of cervical pregnancy evaluated with MRI have been reported in the literature.[47] The fetal pole between the internal and external cervical os appears as a high signal intensity structure with a low signal intensity rim on T2WI [Figure 12]. On contrast administration, the tree-like enhancing solid components and irregularly enhancing peripheral rim can be observed within the hemorrhagic mass.[47,48] Cesarean scar pregnancy is an uncommon form of ectopic pregnancy that demonstrates gestational sac in the lower uterine segment with the bulging of the uterine contour and thinning of the myometrium between the bladder and the gestational sac [Figure 13].

Hydatidiform mole

The hydatidiform mole is seen during pregnancy and could be complete or partial. Complete mole results from fertilizing an empty ovum with one or more sperm, whereas partial

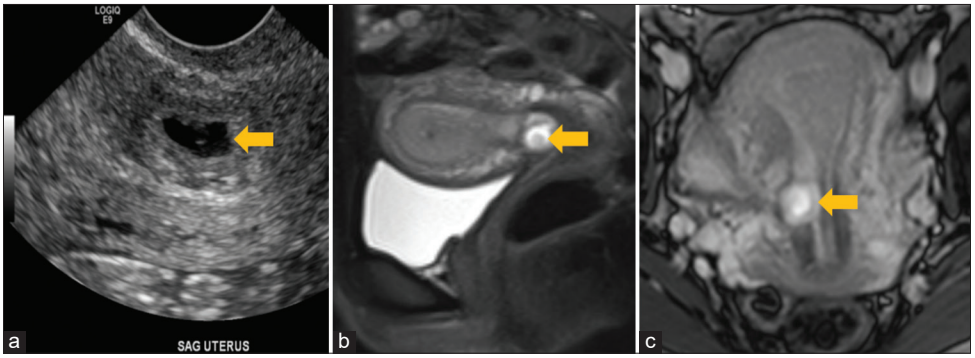

Figure 12: A 22-year-old woman presented with pelvic pain from cervical pregnancy. (a) Grayscale ultrasound image demonstrates an eccentric gestational sac (arrow) centered on the anterior lip of the cervix. (b) Sagittal T2WI and (c) axial T2WI demonstrate a small gestational sac (arrow) centered on the cervix.

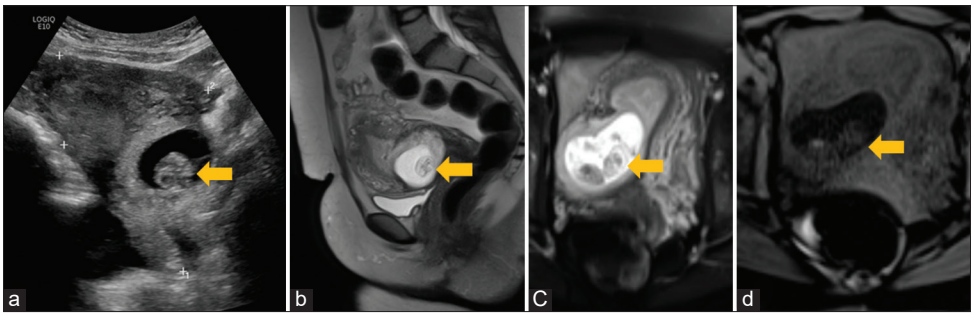

Figure 13: A 26-year-old woman presented with pelvic pain from C-section scar pregnancy. (a) Grayscale ultrasound image demonstrates an eccentric gestational sac (arrow) centered on the lower uterine segment. (b) Axial T2WI, (c) Axial T2WI and (d) Axial T1WI MRI images show a gestational sac with a fetal pole (arrow) centered on the lower uterine segment.

mole results from fertilization between a healthy ovum and more sperm. The prevalence of molar pregnancy in the United States is one for every 1000 pregnancies.[49] The symptoms of the complete mole are vaginal bleeding at 6–16 weeks gestation seen in 46% of cases, enlarged uterus more than expected for the presenting gestational age noticed in 24% of cases, and hyperemesis gravidarum seen in 14% of cases.[50] Ultrasound is the initial investigation of choice in molar pregnancy; however, MRI provides detailed evaluation by early detection, assessment of the extent of invasion, and recurrence.

On MRI, the hydatidiform mole is visualized as an expansile heterogeneous hypointense mass on T1WI and a hyperintense mass on the T2WI.[50,51] Fetal parts may be seen in partial moles but are absent in the case of complete moles. The mass gets enhanced due to hypervascularity and displays multiple cysts within the uterine cavity on post-gadolinium contrast imaging. Hyperintense foci could be seen on T1WI, which represents hemorrhage. On T2WI, the distinction between myometrium and the hydatidiform mole is sharp, indicating the absence of the mole invasion into the myometrium.[50]

Uterine rupture

Uterine rupture can occur spontaneously in an intact unscarred uterus or secondary to uterine scar or after trauma.[52] Scar dehiscence is the incomplete separation of endometrial and myometrial layers with intact serosa. In contrast, uterine rupture is the complete separation of the uterine layers through the serosa and a connection between the uterine and peritoneal cavity.[53] The ultrasound displays non-specific findings like fluid in the peritoneum, whereas MRI provides the ability to assess the uterine wall. Rupture is visualized as the defect area filled with blood leading to a more accurate diagnosis.[53] High signal intensity on T1WI indicates proteinaceous blood contents, which serve the ruptured area. On T2WI, uterine rupture appears as a high signal intensity extending through the uterine wall from the endometrial to the serosal layer [Figures 14 and 15].[54] The T2WI depicts all the involved uterus layers that allow

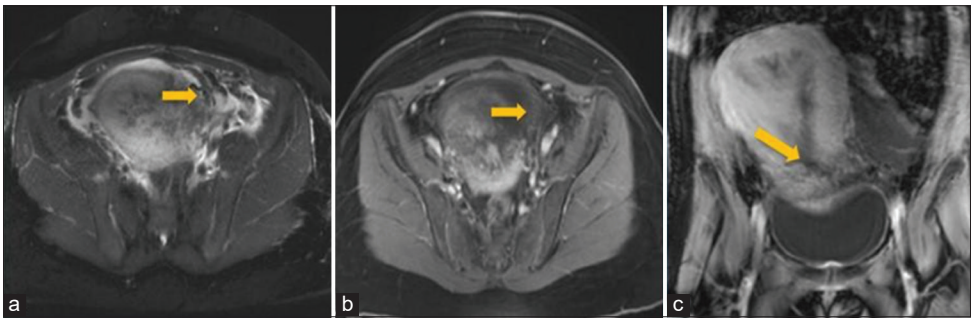

Figure 14: A 58-year-old woman presented with uterine rupture presenting with hypotension and headache. (a) Axial T2 FS shows a defect in the lower uterine segment (arrow) in all layers, including serosa, with marked surrounding edema and fluid. (b) Axial T1 post-contrast fat saturated shows heterogeneous enhancement of the uterus (postpartum state) and defect (arrow). (c) Coronal T1 post-contrast fat saturated shows a defect in the lower segment (arrow).

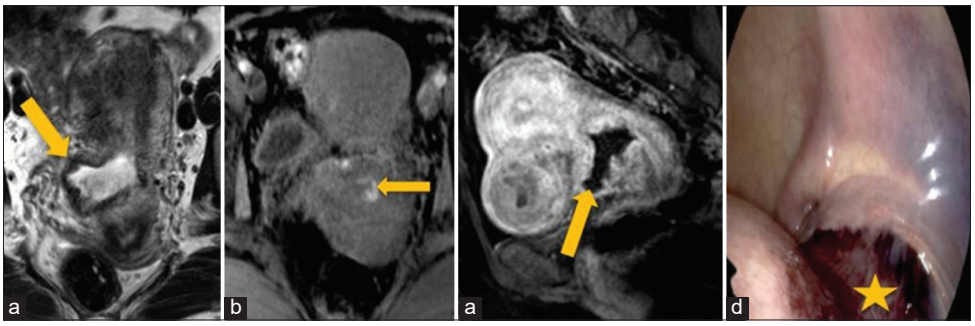

Figure 15: A 34-year-old woman presented with uterine rupture after elective termination of pregnancy with dilatation and curettage and complaints of abdominal pain and bleeding. (a) Axial T2 and (a) axial T1 non-contrast images show expansion of C-section scar (arrow) and internal blood products. (c) Sagittal T1 post-contrast image shows the expansion of the C-section scar (arrow) and internal blood products (star). (d) *In vivo* surgical image showing the uterine rupture (arrow).

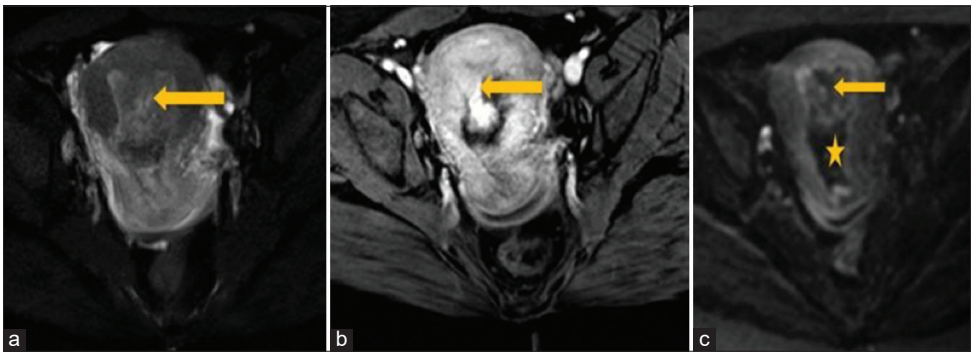

Figure 16: A 56-year-old woman presented with retained products of conception and complains of vaginal bleeding. (a) Axial T2 fat-saturated image shows intermediate T2 signal soft tissue in the uterine fundus (arrow). (b) Axial T1 post-contrast and (c) axial DWI images show irregular enhancing soft tissue in the upper endometrial cavity (arrow) and restricted diffusion consistent with retained products of conception. Notice blood products in the lower uterine cavity (star).

for specific details about laceration, and fetal pole, and distinguishes thrombosed vessels, multiple fibroids, and edema. Sagittal images perpendicular to the scar are more accurate for diagnosis.

RPOC

RPOC can occur after termination of pregnancy or after expected vaginal delivery due to retained placental tissues. It is the second most common cause of postpartum hemorrhage after uterine atony. The occurrence of RPOC after second-trimester delivery (40%) is higher than in other trimesters.[39] On MRI, intracavitary soft tissues with variable intensity and enhancement are noticed in T1, T2, and post-contrast images [Figure 16]. The variability depends on tissue necrosis and hemorrhage.[39] All the above findings overlap with gestational trophoblastic disease results. To assess RPOC without contrast administration, arterial spin labeling MRI can be considered. In this technique, the magnetically labeled water in the blood acts as a contrast, and the intensity of the signal increases with the vascularity of retained tissue.[55] However, this technique could not replace the ultrasound and dynamic contrast MRI, as its efficacy remains unclear.

The spectrum of placenta accreta

Depending on the depth of invasion, three types of placental abnormalities can be described: (i) Placenta accreta, (ii) placenta increta, and (iii) placenta percreta. In the placenta accreta, the villi are attached to but do not invade the myometrium. Placenta percreta is characterized by invading the entire myometrium and the adjacent organs. To improve the management outcomes and pre-operative planning, MRI aids in identifying the placental invasion.

MRI has 94% and 84% sensitivity and specificity in diagnosing the placenta accreta spectrum.[56] The placenta becomes

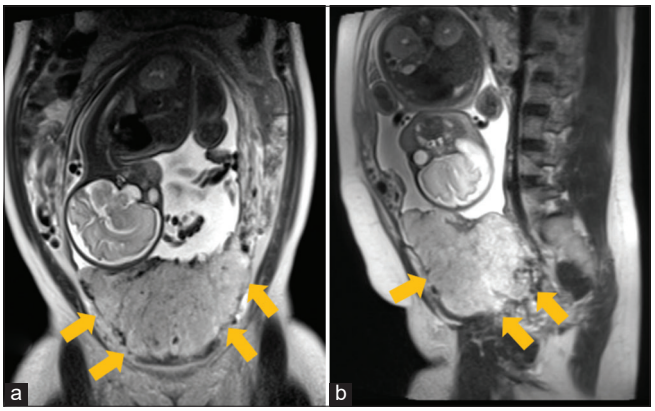

Figure 17: A 38-year-old woman presented for the evaluation of placenta accreta. (a) Coronal T2-weighted image and (b) sagittal T2-weighted MRI images demonstrate gravid uterus with a low-lying placenta previa overlying the cervix. There is loss placental-myometrial interface in the right anterior lower uterine segment (arrows) with evidence of retroplacental bands. There is increased retroplacental vascularity as well.

tethered against the myometrium and exhibits hindered growth with increased gestational age – such tethering results in lumpy placenta with rounded edges that demonstrate direct and indirect signs on imaging. Direct signs include disruptive myometrial trilaminar signal, the focal uterine bulge at the lower uterine segment, and extrauterine involvement. Indirect signs include heterogeneous placental signal intensity, irregular and T2WI hypointense intraplacental bands, proliferative retroplacental uterine and pelvic veins, and hypervascular placenta [Figure 17].[57] However, it should be remembered that any isolated imaging finding might not direct to an accurate diagnosis. Combining findings can improve the ability to diagnose the placenta accreta spectrum. Delli Pizzi *et al.* reported that direct imaging signs and abnormal intraplacental vascularity enhance the sensitivity

and specificity of MRI to 67% and 100%, respectively, while direct imaging signs and myometrial thinning resulted in 100% sensitivity and 77% specificity.[57,58]

CONCLUSION

MR imaging, with its evolving invention of sequences and high sensitivity, is becoming a significant part of an investigation in the emergency room. Manipulating signal intensities, large imaging area, and soft-tissue contrast resolution provide functional and prognostic information. It is essential for radiologists to become more familiar with MRI readings, as this would allow the reader to provide the referring physicians with a more comprehensive report.

Declaration of patient consent

Patient's consent not required as there are no patients in this study.

Financial support and sponsorship

Nil.

Conflicts of interest

There are no conflicts of interest.

REFERENCES

1. Foti PV, Tonolini M, Costanzo V, Mammino L, Palmucci S, Cianci A, *et al.* Cross-sectional imaging of acute gynaecologic disorders: CT and MRI findings with differential diagnosis-part II: Uterine emergencies and pelvic inflammatory disease. Insights Imaging 2019;10:118.
2. Czeyda-Pommersheim F, Kalb B, Costello J, Liau J, Meshksar A, Arif Tiwari H, *et al.* MRI in pelvic inflammatory disease: A pictorial review. Abdom Radiol (NY) 2017;42:935-50.
3. Fahmy HS, Swamy N, Elshahat HM. Revisiting the role of MRI in gynecological emergencies an institutional experience. Egypt J Radiol Nuclear Med 2015;46:769-79.
4. Proscia N, Jaffe TA, Neville AM, Wang CL, Dale BM, Merkle EM. MRI of the pelvis in women: 3D versus 2D T2-weighted technique. American Journal of Roentgenology 2010; 195:254-9.
5. Agrawal G, Sethi I, Oto A. Part I: MR of the female pelvis. Appl Radiol 2012;41:18.
6. Sydow BD, Seigelman ES. Uterine MRI: A review of technique and diagnosis. Appl Radiol 2008;37:18.
7. Cansu A, Bulut E, Dinc G, Bekircavusoglu S, Eyuboglu I, Guven ES, *et al.* Diagnostic efficacy of T2 Dark Spot, T2 dark rim signs, and T2 shading on magnetic resonance imaging in differentiating endometriomas from hemorrhagic cysts. J Comput Assist Tomogr 2019;43:619-22.
8. Parker RA 3rd, Yano M, Tai AW, Friedman M, Narra VR, Menias CO. MR imaging findings of ectopic pregnancy: A pictorial review. Radiographics 2012;32:1445-60.
9. Raptis CA, Mellnick VM, Raptis DA, Kitchin D, Fowler KJ, Lubner M, *et al.* Imaging of trauma in the pregnant patient. Radiographics 2014;34:748-63.
10. Sheikh-Sarraf M, Nougaret S, Forstner R, Kubik-Huch RA. Patient preparation and image quality in female pelvic MRI: Recommendations revisited. European Radiology 2020;30:5374-83.
11. Hase S, Mitsumori A, Inai R, Takemoto M, Matsubara S, Akamatsu N, *et al.* Endometrial polyps: MR imaging features. Acta Med Okayama 2012;66:475-85.
12. Hubert J, Bergin D. Imaging the female pelvis: When should MRI be considered? Appl Radiol 2008;37:9.
13. Ssi-Yan-Kai G, Rivain A-L, Trichot C, Morcelet M-C, Prevot S, Deffieux X, De Laveaucoupet J. What every radiologist should know about adnexal torsion. Emergency Radiology 2018;25:51-9.
14. Pavlik E, DePriest P, Gallion H, Ueland F, Reedy M, Kryscio R, *et al.* Ovarian volume related to age. Gynecologic oncology 2000;77:410-2.
15. Outwater EK, Talerman A, Dunton C. Normal adnexa uteri specimens: Anatomic basis of MR imaging features. Radiology 1996;201:751-5.
16. Outwater EK, Mitchell DG. Normal ovaries and functional cysts: MR appearance. Radiology 1996;198:397-402.
17. Grover SB, Antil N, Katyan A, Rajani H, Grover H, Mittal P, *et al.* Niche role of MRI in the evaluation of female infertility. Indian J Radiol Imaging 2020;30:32-45.
18. Soper DE. Pelvic inflammatory disease. Obstet Gynecol 2010;116:419-28.
19. Revzin MV, Mathur M, Dave HB, Macer ML, Spektor M. Pelvic inflammatory disease: Multimodality imaging approach with clinical-pathologic correlation. Radiographics 2016;36:1579-96.
20. Roche O, Chavan N, Aquilina J, Rockall A. Radiological appearances of gynaecological emergencies. Insights Imaging 2012;3:265-75.
21. Stenchever M. History, physical examination, and preventive health care. In: Comprehensive Gynecology. 4th ed. St Louis, MO: Mosby; 2001. p. 137-54.
22. Foti PV, Attinà G, Spadola S, Caltabiano R, Farina R, Palmucci S, *et al.* MR imaging of ovarian masses: Classification and differential diagnosis. Insights Imaging 2016;7:21-41.
23. Duarte AL, Dias JL, Cunha TM. Pitfalls of diffusion-weighted imaging of the female pelvis. Radiol Bras 2018;51:37-44.
24. Li W, Zhang Y, Cui Y, Zhang P, Wu X. Pelvic inflammatory disease: Evaluation of diagnostic accuracy with conventional MR with added diffusion-weighted imaging. Abdom Imaging 2013;38:193-200.
25. Thomassin-Naggara I, Daraï E, Nassar-Slaba J, Cortez A, Marsault C, Bazot M. Value of dynamic enhanced magnetic resonance imaging for distinguishing between ovarian fibroma and subserous uterine leiomyoma. J Comput Assist Tomogr 2007;31:236-42.
26. Singh AK, Desai H, Novelline RA. Emergency MRI of acute pelvic pain: MR protocol with no oral contrast. Emerg Radiol 2009;16:133-41.
27. Deshmukh SP, Gonsalves CF, Guglielmo FF, Mitchell DG. Role of MR imaging of uterine leiomyomas before and after embolization. Radiographics 2012;32:E251-81.
28. Agostinho L, Cruz R, Osório F, Alves J, Setúbal A, Guerra A.

MRI for adenomyosis: A pictorial review. Insights Imaging 2017;8:549-56.
29. Bourgioti C, Preza O, Panourgias E, Chatoupis K, Antoniou A, Nikolaidou ME, *et al.* MR imaging of endometriosis: Spectrum of disease. Diagn Interv Imaging 2017;98:751-67.
30. Bazot M, Darai E, Hourani R, Thomassin I, Cortez A, Uzan S, *et al.* Deep pelvic endometriosis: MR imaging for diagnosis and prediction of extension of disease. Radiology 2004;232:379-89.
31. Stratton P, Winkel C, Premkumar A, Chow C, Wilson J, Hearns-Stokes R, *et al.* Diagnostic accuracy of laparoscopy, magnetic resonance imaging, and histopathologic examination for the detection of endometriosis. Fertil Steril 2003;79:1078-85.
32. Corwin MT, Gerscovich EO, Lamba R, Wilson M, McGahan JP. Differentiation of ovarian endometriomas from hemorrhagic cysts at MR imaging: Utility of the T2 dark spot sign. Radiology 2014;271:126-32.
33. Salim S, Won H, Nesbitt-Hawes E, Campbell N, Abbott J. Diagnosis and management of endometrial polyps: A critical review of the literature. J Minim Invasive Gynecol 2011;18:569-81.
34. Balcacer P, Cooper KA, Huber S, Spektor M, Pahade JK, Israel GM. Magnetic resonance imaging features of endometrial polyps: frequency of occurrence and interobserver reliability. J Comput Assist Tomogr 2018;42:721-6.
35. Giurazza F, Corvino F, Silvestre M, Cavaglià E, Amodio F, Cangiano G, *et al.* Uterine Arteriovenous Malformations. Amsterdam, Netherlands: Proceedings of the Seminars in Ultrasound, CT and MRI, Elsevier; 2021. p. 37-45.
36. Cura M, Martinez N, Cura A, Dalsaso TJ, Elmerhi F. Arteriovenous malformations of the uterus. Acta Radiol 2009;50:823-9.
37. Grivell RM, Reid KM, Mellor A. Uterine arteriovenous malformations: A review of the current literature. Obstet Gynecol Surv 2005;60:761-7.
38. Iraha Y, Okada M, Iraha R, Azama K, Yamashiro T, Tsubakimoto M, *et al.* CT and MR imaging of gynecologic emergencies. Radiographics 2017;37:1569-86.
39. Sellmyer MA, Desser TS, Maturen KE, Jeffrey RB Jr., Kamaya A. Physiologic, histologic, and imaging features of retained products of conception. Radiographics 2013;33:781-96.
40. Bookwalter CA, VanBuren WM, Neisen MJ, Bjarnason H. Imaging appearance and nonsurgical management of pelvic venous congestion syndrome. Radiographics 2019;39:596-608.
41. Knuttinen MG, Xie K, Jani A, Palumbo A, Carrillo T, Mar W. Pelvic venous insufficiency: Imaging diagnosis, treatment approaches, and therapeutic issues. AJR Am J Roentgenol 2015;204:448-58.
42. Cimsit C, Yoldemir T, Tureli D, Aribal ME. Evaluation of sacroiliac joint MRI for pelvic venous congestion signs in women clinically suspected of sacroiliitis. Acta Radiol 2017;58:849-55.
43. Leiber LM, Thouveny F, Bouvier A, Labriffe M, Berthier E, Aubé C, *et al.* MRI and venographic aspects of pelvic venous insufficiency. Diagn Interv Imaging 2014;95:1091-102.
44. Yang DM, Kim HC, Nam DH, Jahng GH, Huh CY, Lim JW. Time-resolved MR angiography for detecting and grading ovarian venous reflux: Comparison with conventional venography. Br J Radiol 2012;85:e117-22.
45. Rha SE, Byun JY, Jung SE, Jung JI, Choi BG, Kim BS, *et al.* CT and MR imaging features of adnexal torsion. Radiographics 2002;22:283-94.
46. Si MJ, Gui S, Fan Q, Han HX, Zhao QQ, Li ZX, *et al.* Role of MRI in the early diagnosis of tubal ectopic pregnancy. Eur Radiol 2016;26:1971-80.
47. Jung SE, Byun JY, Lee JM, Choi BG, Hahn ST. Characteristic MR findings of cervical pregnancy. J Magn Reson Imaging 2001;13:918-22.
48. Le T, Poder L, Deans A, Joe BN, Laros RK Jr., Coakley FV. Magnetic resonance imaging of cervical ectopic pregnancy in the second trimester. J Comput Assist Tomogr 2012;36:249-52.
49. Lin LH, Polizio R, Fushida K, Francisco RP. Imaging in gestational trophoblastic disease. Semin Ultrasound CT MR 2019;40:332-49.
50. Shaaban AM, Rezvani M, Haroun RR, Kennedy AM, Elsayes KM, Olpin JD, *et al.* Gestational trophoblastic disease: Clinical and imaging features. Radiographics 2017;37:681-700.
51. Herek D, Karabulut N. The role of magnetic resonance imaging in the diagnosis of complete hydatidiform mole in a twin pregnancy. Int J Gynaecol Obstet 2013;123:77.
52. Hruska KM, Coughlin BF, Coggins AA, Wiczyk HP. MRI diagnosis of spontaneous uterine rupture of an unscarred uterus. Emerg Radiol 2006;12:186-8.
53. Alamo L, Vial Y, Denys A, Andreisek G, Meuwly JY, Schmidt S. MRI findings of complications related to previous uterine scars. Eur J Radiol Open 2018;5:6-15.
54. Paspulati RM, Dalal TA. Imaging of complications following gynecologic surgery. Radiographics 2010;30:625-42.
55. Kosaka N, Fujiwara Y, Kurokawa T, Matsuda T, Kanamoto M, Takei N, *et al.* Evaluation of retained products of conception using pulsed continuous arterial spin-labeling MRI: Clinical feasibility and initial results. MAGMA 2018;31:577-84.
56. Kilcoyne A, Shenoy-Bhangle AS, Roberts DJ, Sisodia RC, Gervais DA, Lee SI. MRI of placenta accreta, placenta increta, and placenta percreta: pearls and pitfalls. AJR Am J Roentgenol 2017;208:214-21.
57. Brown BP, Meyers ML. Placental magnetic resonance imaging Part II: Placenta accreta spectrum. Pediatr Radiol 2020;50:275-84.
58. Delli Pizzi A, Tavoletta A, Narciso R, Mastrodicasa D, Trebeschi S, Celentano C, *et al.* Prenatal planning of placenta previa: Diagnostic accuracy of a novel MRI-based prediction model for placenta accreta spectrum (PAS) and clinical outcome. Abdom Radiol (NY) 2019;44:1873-82.

How to cite this article: Gopireddy DR, Virarkar M, Kumar S, Vulasala SS, Nwachukwu C, Lamsal S. Acute pelvic pain: A pictorial review with magnetic resonance imaging. J Clin Imaging Sci 2022;12:48.